Topological Signatures For Fast Mobility Analysis

Abhirup Ghosh, Benedek Rozemberczki, [†]Subramanian Ramamoorthy, Rik Sarkar
School of Informatics, University of Edinburgh, U.K.
abhirup.ghosh@ed.ac.uk, benedek.rozemberczki@ed.ac.uk, s.ramamoorthy@ed.ac.uk, rsarkar@inf.ed.ac.uk
[†]FiveAI Ltd. Edinburgh, U.K. s.ramamoorthy@five.ai

ABSTRACT

Analytic methods can be difficult to build and costly to train for mobility data. We show that information about the topology of the space and how mobile objects navigate the obstacles can be used to extract insights about mobility at larger distance scales. The main contribution of this paper is a topological signature that maps each trajectory to a relatively low dimensional Euclidean space, so that now they are amenable to standard analytic techniques. Data mining tasks: nearest neighbor search with locality sensitive hashing, clustering, regression, etc., work more efficiently in this signature space. We define the problem of mobility prediction at different distance scales, and show that with the signatures simple k nearest neighbor based regression perform accurate prediction. Experiments on multiple real datasets show that the framework using topological signatures is accurate on all tasks, and substantially more efficient than machine learning applied to raw data. Theoretical results show that the signatures contain enough topological information to reconstruct non-self-intersecting trajectories upto homotopy type. The construction of signatures is based on a differential form that can be generated in a distributed setting using local communication, and a signature can be locally and inexpensively updated and communicated by a mobile agent.

CCS CONCEPTS

• **Mathematics of computing → Algebraic topology**; • **Information systems → Location based services**; **Geographic information systems**; **Sensor networks**; • **Theory of computation → Nearest neighbor algorithms**; • **Computing methodologies → Machine learning approaches**;

KEYWORDS

Trajectory analysis, mobility analysis, near neighbor search, clustering, computational topology, differential forms, sketches, streaming

ACM Reference Format:
Abhirup Ghosh, Benedek Rozemberczki, [†]Subramanian Ramamoorthy, Rik Sarkar. 2018. Topological Signatures For Fast Mobility Analysis. In *26th ACM SIGSPATIAL International Conference on Advances in Geographic Information Systems (SIGSPATIAL '18), November 6–9, 2018, Seattle, WA, USA.* ACM, New York, NY, USA, 10 pages. https://doi.org/10.1145/3274895.3274952

SIGSPATIAL '18, November 6–9, 2018, Seattle, WA, USA
© 2018 Association for Computing Machinery.
ACM ISBN 978-1-4503-5889-7/18/11…$15.00
https://doi.org/10.1145/3274895.3274952

1 INTRODUCTION

Location traces are computationally challenging to process. Distances between trajectories like Fréchet and Hausdorff distances [3] do not form a normed space, Dynamic time warping distance [29] does not even form a metric [14]. As a result, typical computational methods are difficult to apply. Specialized techniques have been developed for location traces. Theoretical approaches such as locality sensitive hashing have to be tailored to trajectories for faster near neighbor search [4, 14, 20]; computation of medians [7], popular paths [21] etc have also been considered.

Analysis and prediction of motion have been developed with Markov models [24, 35, 38] that assume motion to depend only on the current "state" of an agent and not on longer history. However, recent experimental results show that the memoryless assumption of Markov models does not hold in real location data, since agents do not execute a random walk, but move with the purpose to reach a destination [32]. Specialized neural network based models [25, 34] with the power to encode longer history are shown in practice to be effective for next road segment prediction, although they do not provide rigorous models for other general tasks, e.g., search and comparison of trajectories. We instead seek a framework for interpretable encoding of large scale properties of trajectories, that is compatible with a range of analytic methods.

The motion of objects is determined by the major obstacles in the plane, which defines the geometry and topology of the space. However, considerations of topology raise complex issues, and traditional quantities like Fréchet distance are prohibitively expensive to compute in domains with obstacles [9]. Geometric algorithms thus usually assume motion in a simple plane, or of same topological type.

In past work, Hodge theory and relative homology from algebraic topology have been used for the purpose of topological classification [28, 36]. However, these approaches are only applicable to specific start and end points of trajectories, and yield only discrete classifications by homotopy type, which is not general enough for use in further analysis. They are also expensive to compute. We intend to overcome these obstacles by using more flexible topological constructs.

Our contributions. This paper shows that topological information can enhance mobility analysis by meaningfully encoding large scale patterns of movement, and demonstrates how the relevant information can be represented compactly.

The geometry and topology of the space of mobility itself can be discretized as a graph, where regions of zero or little activity are treated as obstacles or *holes*, and the remaining space is triangulated based on a suitable set of vertices.

Let us define a *discrete differential form* $\xi : E \longrightarrow \mathbb{R}$ as a function that assigns values to directed edges. For any directed edge ab, the function ξ satisfies $\xi(ab) = -\xi(ba)$, that is, the values on an edge and its reverse are negations of each other (See Section 2). Further, the values on the edges sum to zero around any face of the graph, except possibly the obstacles. For each obstacle i, we define a differential form ξ_i such that around obstacle i, ξ_i on the edges sum to 1, and thus preserves topological information with respect to this obstacle.

For any mobility trace A, the differential form values along its directed edges are added to obtain $\xi_i(A)$. For a trajectory that goes around an obstacle i, $\xi_i(A) = 1$. In a space with k obstacles, the general differential form $\xi = \{\xi_1, \xi_2, \ldots \xi_k\}$ is a vector of length k.

The significant property here is that a signature element $\xi_i(A)$ can have a real numbered value when A is not a perfect loop. The signature $\xi(A) \in \mathbb{R}^k$ is a point in k dimensional space. Thus, beyond simple topological equality, the signatures can represent topological *similarity*. The mapping to a normed space enables standard analytic techniques like clustering, regression, density estimation, etc. We discuss the basic construction in Section 3 and the detailed technique in Section 4.

Summations over differential forms preserve only large scale properties, and are insensitive to noise that does not change topological type of a trajectory. As a result, the signatures are invariant to localization errors and GPS noise. They are compact compared to real trajectory data, and can be easily exchanged between mobile nodes to perform mobility comparison among nearby nodes. It is efficient to compute and to update incrementally as an object moves in the plane. Comparison between trajectories is now reduced to comparison of points in a low dimensional space. The signature of a simple trajectory contains sufficient information to provably reconstruct it upto homotopy equivalence.

The knowledge of global topological behaviors of trajectories can be used to make predictions at larger scale beyond the next road segment. For this purpose, we define a notion of prediction at an arbitrary scale r. Simple k nearest neighbor regression on the signatures performs comparably to expensive and opaque neural network based methods, which suggests that the topological features are essential to understanding and prediction of motion.

Data mining techniques of locality sensitive hashing, dimension reduction, etc run efficiently and accurately on the signatures (Section 5). Experiments (Section 6) show that the dimensionality of the signatures can be reduced by selecting only a few obstacles from the domain, and this further increases the efficiency of the system. Based on how the trajectories traverse the domains, the obstacles themselves can be characterized by how they influence mobility.

Section 7 discusses some related works and how the new approach compares with them.

Before we move on with technical details, let us summarize our approach into the following steps: 1. Find obstacle as sparse regions of the plane 2. construct a differential 1-form for each obstacle. 3. As a mobile agent moves, use these forms to track how it circumnavigates each obstacle and get a point in Euclidean space, where each dimension represents behavior with respect to one obstacle. 4. Apply efficient analytic techniques treating trajectories as points in Euclidean space.

2 THEORETICAL BACKGROUND

Discrete differential forms and exterior calculus are a varied topic of study across many disciplines. This section presents a brief description of the main ideas relevant. A more formal treatment can be found in [19]. Readers familiar with the topic can consider skipping ahead to the next section.

Let us represent the space of motion using a simplicial complex or a cell complex. A two dimensional *simplicial complex* is a planar graph G with 0, 1, and 2 dimensional simplices as vertices, edges, and triangles as shown in Figure 1(a). A simplicial complex is built by attaching simplices together along subsimplices.

Orientation of a simplex is defined using ordering of constituent lower dimension simplices. E.g. ordering of two 0−simplices $[v_0, v_1]$ produces an oriented 1−simplex or a directed edge, e, while its opposite orientation is $-[v_0, v_1]$ or $-e$.

A linear combination of d dimensional simplices: $\sum_{i=0}^{k} \lambda_i \sigma_i$, where each λ_i is an integer, is called a d-chain. A trajectory or mobility trace can be seen as 1-chain.

The boundary ($\partial\sigma$) of an oriented p−chain σ is a $(p-1)$−chain that separates σ from rest of the complex and the orientation of the boundary is inherited from σ. Planar graphs are orientable, meaning that all its simplices can be oriented consistently [23]. Here, all 2−simplices or faces are assumed to be oriented counter clockwise. Consequently, the boundary of a summation of faces (2-chains) is the sum of their boundaries (1-chains); formally: $\partial(f_1 + f_2 + f_3 + \ldots) = \partial f_1 + \partial f_2 + \partial f_3 + \ldots$ (Figure 1(b)).

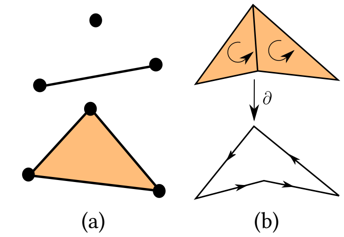

Figure 1: (a) $0, 1,$ **and** $2-$**simplices (b) Boundary operation on a chain of** 2**-simplices**

Cell complexes are a natural extension of simplicial complexes. The only difference meaningful to this context is that a two dimensional cell, or face, can be a simple polygon instead of a triangle, otherwise a cell complex retains all relevant properties of a simplicial complex. The area external to the planar graph is called the exterior face, or the *face at infinity*. The edges at the boundary of this face constitute the exterior boundary.

Dual complex. The dual of a simplicial complex G is a planar graph $\star G$ where a face σ in G corresponds to a node $\star\sigma$ in $\star G$ and an edge $\star e$ in $\star G$ exists between two nodes if the corresponding two faces in G are adjacent with shared edge e. An example is shown in Figure 2(a).

2.1 Discrete differential 1-forms and co-chains

Differential forms are defined as functions over the directed cells of the cell complex. Specifically, 1-forms are values for the edge set

E of a graph as $\omega : E \longrightarrow \mathbb{R}$. The values are associated with directed edges, so that $\omega(ab) = -\omega(ba)$. Given a discrete trace written as $e_1 + e_2 + e_3 \ldots$, the integral of the form over it is now computed as sum of ω over the directed edges: $\omega(e_1) + \omega(e_2) + \omega(e_3) \ldots$.

The function ω thus defines a co-chain in $C^1(G; \mathbb{R})$ that maps 1-chains to real values. The entire construct translates to a dual with a dual function $\star\omega$ defined simply as $\star\omega(\star e) = \omega(e)$. Thus $\star\omega$, yields a differential form ω, which will be useful in the following section.

Sources and sinks. Suppose $X(v)$ is the set of edges of the type $(v, \circ)$ – that is, all edges incident on v, with orientation selected as pointing outward from v. Then we can compute the net *outflow* from v as $h(v) = \sum_{e \in X(v)} \omega(e)$. Depending on this value, v can be a:

- **Source:** net outflow $h(v) > 0$.
- **Internal or regular node:** net outflow $h(v) = 0$.
- **Sink:** net outflow $h(v) < 0$.

Observe the effect on the dual system. For a primal face f with dual vertex $\star f$, we have : $\sum_{\star e \in X(\star f)} \star\omega(\star e) = \omega(\partial f)$.

3 TOPOLOGICAL SIGNATURES

The goal is to utilize differential forms to characterize the behavior of the traces with respect to obstacles in the domain. We assume that the obstacles such as buildings and lakes reside in the larger faces of the graph and the mobile objects move along the nodes and edges of the graph. The question of what constitutes important obstacles in a domain will be taken up later, for now assume that some faces are given to us to be treated as obstacles.

Dual sources. Each obstacle is a source of a dual vector field $\star\xi$. More specifically, given a face f with an obstacle, the corresponding dual node $\star f$ is the only source for $\star\xi$ in the dual graph. The external face, dual node $\star f_0$ is the only sink. A specific weight $h(\star f)$, usually set to 1, is associated with each source $\star f$.

The dual form with a value for each directed dual edge defines a differential form for the primal graph using $\xi(e) = \star\xi(\star e)$. For each face f_i that is an obstacle, we create one such differential form ξ_i, which equivalently sums to $h(\star f_i)$ around the boundary ∂f – representing a cyclic vector field along ∂f. We refer to these as the *signature forms* for the obstacles. The idea is shown in Figure 2.

The important property of this structure is that over any cycle γ surrounding f, the form sums to $\xi(\gamma) = \xi(\partial f) = h(\star f)$.

Theorem 3.1. *For a 2−chain U with coefficients in* 0, 1 *in G (excluding f_0) with a single source face f_i, the differential form $\xi(\partial U) = h(\star f_i)$ if $f_i \in U$, otherwise $\xi(\partial U) = 0$.*

The proof follows simply from the fact that for any face f, $\xi(\partial f) = h(\star f)$, and that $\partial(f_1 + f_2 + f_3 + \ldots) = \partial f_1 + \partial f_2 + \partial f_3 + \ldots$.

Topological signatures of trajectories. Using these differential forms, we can now define the topological signature of a trace. If there are k obstacles and corresponding signature forms, then for a trace T, we get a k dimensional vector $\theta(T)$. The component $\theta_i(T)$ represents to what extent T goes around obstacle i. If it forms exactly one complete cycle, then $\theta_i(T) = h(f_i)$.

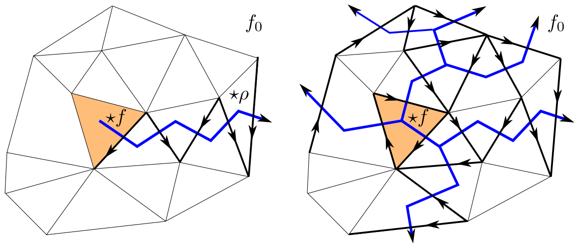

(a) (b)

Figure 2: (a) An example primal graph with a source face f. Dual path $\star\rho$ flows from $\star f$ to external node $\star f_0$.(b) Multiple dual paths from the source $\star f$ construct a differential form of non-zero integral around $\star f$.

The useful feature here is that even if T does not quite form a cycle, $\theta_i(T)$ still reveals valuable information. If the value of $\theta_i(T)$ is higher, it implies that t goes farther around the obstacle. This construction is more general than simple winding numbers, since the differential forms construction can assign arbitrary weights to individual edges, and can be made sensitive to specific mobile agents. From a computational point of view, it works directly on a discrete structure, with or without knowledge of locations. The symmetric nature of directed edges nullifies the effect of noisy GPS localization.

The signature $\theta : \mathcal{T} \longrightarrow \mathbb{R}^k$ maps trajectories in set $\mathcal{T}$ to a k dimensional space.

4 ALGORITHMS

This section describes how the mathematical construct of discrete topological signatures can be realized, including in a distributed environment.

4.1 Construction of planar graphs

The algorithms work on any planar graph on the mobility domain. Following are a few possible strategies varied by availability of mobility data and infrastructure.

Graphs from data. In many scenarios, road map data is available and directly yields a graph, where road intersections are vertices and road segments are edges. Alternatively, a simple model – a grid or a triangulation of randomly deployed point sets (vertices) may serve as the planar graph. In [28] a triangulation of the locations from the dataset itself is used as the discrete domain. A mobile trace is then converted to a sequence of edges in this graph. This can be done by simply mapping locations to nearby vertices. With sufficient data, it is also possible to construct a roadmap itself as is done in openstreetmap and other projects [8].

Discrete sensor domains. In sensor networks and robotics, trajectories may be recorded by sensors. Such a trajectory may not have any localization at all, and is represented simply as a sequence of sensors that have detected the mobile object. For localized and unlocalized wireless sensor networks, there is a large body of research in topology control, localization and planar graph extraction, relying on the locality of wireless transmission. Depending on the network, such a technique can compute planar graph of the nodes [16, 31].

Our differential forms setup, as described in the previous section, works on the planar graph, without the need for an explicit embedding.

4.1.1 Obstacles and dual sources. Having constructed the planar graph and map of trajectories to sequence of edges, we are left with the question of what are the 'obstacles' in the domain. In principle, every face can be an obstacle, but this is neither intuitive, nor informative to any algorithm operating on the data.

Instead, a face can be an obstacle if it is larger than a certain size, measured as area, diameter, or some other measure. The strength $h(\star f)$ of the source $\star f$, which is normally set to 1, can also be set to be proportional to the measure to reflect the weight of an obstacle. In unlocalized scenarios, there are techniques for detecting boundaries of large enough sizes [33], while a measure such as the number of edges on the face can be used to determine its weight.

Subsection 5.3 discusses more involved questions of determining the importance of an obstacle and dimension reduction techniques to merge nearby obstacles to simplify data.

4.2 Constructing signature forms

For each obstacle face f, our basic strategy is to take its dual face $\star f$, and start multiple walks in the dual graph. The walks spread in all directions, and end in the exterior face at infinity $\star f_0$. The total weight of the walks is $h(\star f_i)$. Having constructed walks of total weight of $h(\star f_i)$, the weight of each dual edge can be transferred to the corresponding primal edge as $\xi_i(ab) := \star\xi_i(\star ab)$.

In a distributed sensor network scenario, the operations of a dual node $\star f$, which is a face f in the primal, can be handled by an elected sensor node on its boundary. There are different ways to structure these walks and the corresponding differential form. Unless mentioned otherwise, the following mechanisms work in localized as well as unlocalized graphs.

Random walk in the dual. Starting from the dual node $\star f_i$, create several random walks that stop only when they reach $\star f_0$. Each walk has a weight w, and to each directed dual edge $\star ab$ it traverses, the weight is added as $\star\xi_i(\star ab) := \star\xi_i(\star ab) + w$. Note that this process preserves the strictly one source $(\star f_i)$ and one sink $(\star f_0)$ since at every other vertex it exits every time it enters. The walk is also allowed to pass through $\star f_i$ as well as any other dual vertex.

Shortest paths in the dual. Another possible way of constructing the signature forms is using shortest paths to the boundary faces, which are adjacent to the external face f_0.

From these boundary faces, select a subset either randomly or at some uniform separation. From the dual source node $\star f_i$, a shortest path in the dual is computed to each such boundary face $\star f_j$ and appended a final edge $(\star f_j, \star f_0)$ to complete the walk.

Following a straight line to the boundary. In scenarios with available locations, instead of selecting faces at the boundary, it is possible to select specific locations at the boundary and follow a straight line to them. By picking a location to place the dual nodes inside faces, e.g., at centroids, a line starts from a source location $\star f_i$. 'Following' a straight line in the dual graph is essentially choosing the next node in the path that minimizes the distance to the line segment [27].

4.3 Computing topological signatures

A trace consists of a sequence of edges, and for each edge e, the value $\xi_i(e)$ is computed corresponding to each obstacle i. Thus, for each e traversed by the trajectory T results in updates of the form $\theta_i(T) = \theta_i(T) + \xi_i(e)$.

In a distributed scenario, this works naturally, where for any edge ab, the ξ values for this edge are held by sensors a and b, and when a mobile object traverses this edge, it can obtain the values locally and maintain its own $\theta(T)$ vector. Or in a tracking scenario, the sensors as they track the object's motion can maintain and handoff this value.

While in principle $\theta_i(T)$ can take up any real value, the larger values of θ imply an agent circumscribing an obstacle many times. This is unlikely in many realistic scenarios such as trips in a city. In such cases, it is natural to assume that on a single trip an agent does not take sub-optimal self-intersecting paths that that go all the way around the obstacle. Thus, for such trajectories, for any obstacle i, $|\theta_i(T)| < 1$, and let us refer them as simple trajectories. Theorem 4.1 shows that for simple trajectories, the signature uniquely determines their homotopy type.

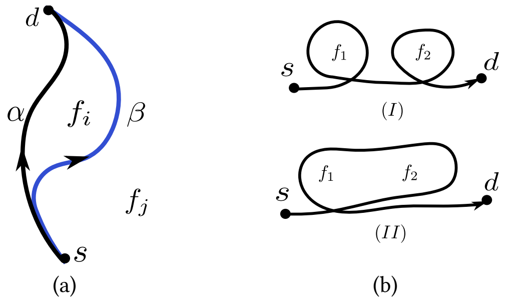

Figure 3: (a)Two simple trajectories α, β goes from s to d have same homotopy type w.r.t. source f_j, but different homotopy type w.r.t. f_i. (b) Two self-intersecting paths between same source and destination may have same signature value but different homotopy type.

Theorem 4.1. *For two simple trajectories α and β between same source s and destination d:*

$$\theta_i(\alpha) = \begin{cases} \theta_i(\beta) \text{ If } \alpha, \beta \text{ have same homotopy w.r.t. source } f_i. \\ \theta_i(\beta) \pm 1, \text{ otherwise [assuming } h(\star f) = 1] \end{cases}$$

Proof. An example setup is shown in Figure 3(a). Where paths α and β have the same homotopy type with respect to f_j and different types with respect to f_i. The concatenation of α with $-\beta$ gives loop $\gamma = \alpha - \beta$.

The first claim simply says $\theta_j(\alpha) = \theta_j(\beta)$, since otherwise $\theta_j(\alpha - \beta) \neq 0$, contradicts Theorem 3.1.

For the second claim, any closed oriented one dimensional loop object $\hat{\gamma}$ in the two dimensional cell complex is the boundary ∂U of a chain U with coefficients in $[0, 1]$. Thus $f_i \in U$ implies $\xi(\hat{\gamma}) = 1$.

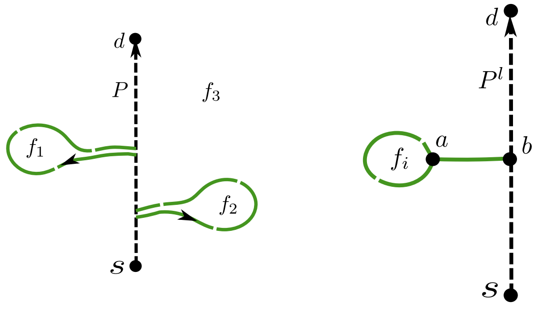

(a) (b)

Figure 4: (a) Construction of homotopy equivalent path for desired signature value. (b) Realization of the idea by taking a path from the current path to the boundary of the obstacle.

Depending on the orientation of $\gamma = \alpha - \beta, \theta(\alpha - \beta) = \pm\theta(\hat{\gamma}) = \pm 1$, implying the second claim. □

Figure 3(b) shows an example where the above condition is violated, and trajectories of the same signature have different homotopy types.

4.4 Reconstructing traces from signatures

The following lemmas say that given a signature it is possible to check in polynomial time if such a trajectory exists, and if so it can be reconstructed up to homotopy equivalence in linear time.

Lemma 4.2. *Given a signature vector X, source s, and destination d; it is possible to find in linear time if there exists a homotopy class of simple paths going from s to d with the signature X.*

Proof. Consider the shortest path P from s to d as shown in Figure 4(a) and its signature $\theta(P)$. Using the result from Theorem 4.1, the only thing to test is if $(\theta_i(P) - X_i) \in \{0, 1, -1\}$ for all i. This can be done in linear time in the number of holes in the domain. □

Lemma 4.3. *Given signature vector X, source s, and destination d, there exists an algorithm to find a unique simple trajectory up to homotopy equivalence with signature X. The algorithm runs in linear time in the number of holes in the domain.*

Proof. A natural extension of Lemma 4.2 uniquely identifies the source faces f_i where we need to change the side by which P passes f_i – precisely where $(\theta_i(P) - X_i) \neq 0$. Next, these sources are fixed iteratively.

Initialize this process by setting the path P as the shortest path from s to d. Suppose at iteration l, the path is P^l and the next obstacle to fix is f_i. Consider an arbitrary node $b \in P^l$, and another arbitrary node $a \in \partial f_i$ as shown in Figure 4(b). Now P^{l+1} is the concatenation of the following path segments: s to b, b to a, a to a (along ∂f_i), a to b, and finally b to d. So, the path P^{l+1} has now right homotopy type w.r.t. f_i. □

This construction essentially determines the homotopy type from the signature. Given that, we can now compute a short path in that class using well known algorithms in computational geometry [18].

5 APPLICATIONS AND OPTIMIZATIONS

Here we discuss how they can be designed and implemented for better applied analytics.

5.1 Nearest neighbor search and Locality Sensitive Hashing

A fundamental question in data analysis is the search for nearest neighbor, or k nearest neighbors, which forms the basis of several classification and clustering techniques and queries on noisy data. In case of trajectories, searching for nearest neighbors is expensive due to the fundamental cost of comparing two long trajectories [3].

Locality sensitive hashing (LSH) is used in data mining to accelerate the search for nearest neighbors. However, defining LSH for trajectories is a non trivial problem, as is constructing computationally efficient hash functions [14]. We want to instead use representations of trajectories as points in the Euclidean space, where good LSH techniques are known.

A standard LSH scheme [11] uses a hash function h constructed as follows. Select a random straight line in $\mathbb{R}^k$. Then project each data point linearly onto the line. Partition the line into segments of length w for some given w, and treat each segment as a "bucket". Nearby data points are likely to hash into the same bucket, while far apart points are likely to hash to different ones. Given a query point q, we can perform the same projection and hashing, and then search for its nearest neighbor in the bucket containing q. Expensive methods [3] can be used for this search since the pruned candidate set is smaller. Repeating the process with multiple hash functions increases the probability to find the true nearest neighbor of q. Note that Euclidean hash is substantially more efficient than direct locality sensitive hashing of trajectories described in [14, 20].

5.2 Predicting motion at large scales

Let us define motion prediction at scale r, where r is a given distance – e.g. 500 meters. We wish to ask where will a mobile object be, when it is at a distance r from its current location. Formally suppose o is the current location, C_r is the circle of radius r centered at o. Based on our mobility data, we can predict p on C_r as a point where the object's trajectory will exit (intersect) C_r.

To measure the error in prediction, suppose the object actually exits the circle at point z. The prediction error is defined as the angle $\phi = \angle poz$. More accurately, it is $\min(|\phi|, |2\pi - \phi|)$. See Figure 5(d). Since the scale itself is given, the essential task here is to predict the right direction from o at scale r, which is represented as predicting the angle.

The motion prediction itself can proceed according to any machine learning method. Experiments in 6 finds that standard prediction techniques based on k-nearest neighbors, linear regression, random forest, gradient boosting trees work well.

5.3 Dimension reduction, correlation and domain analysis

Given that the trajectories are now points in k dimensional Euclidean space given by $\theta(T)$, standard analytic techniques can be applied to better understand the trajectories, and to understand the

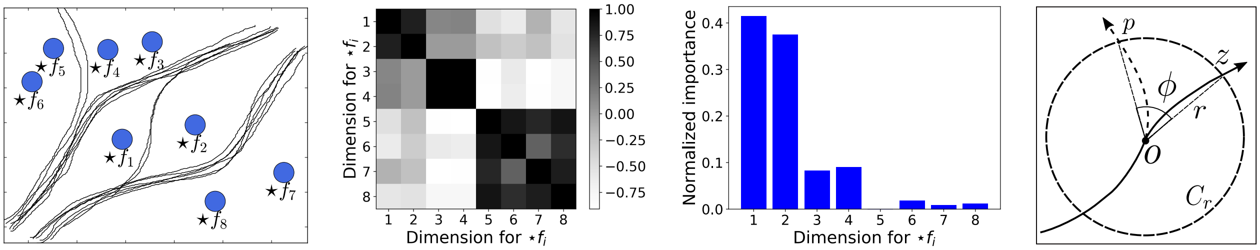

(a) (b) (c) (d)

Figure 5: (a) Trajectory set with 8 obstacles. (b) Correlation matrix with respect to signatures of the trajectories. Darker shades imply higher correlation (c) PCA based importance ranking. (d) Given the history predict the next direction ϕ at current location p.

the underlying domain from the perspective of the given trajectories. We can ask, which obstacles are important, or which obstacles are similar with respect to actual mobility patterns?

Figure 5(a) shows a set of trajectories moving in the plane around obstacles $1, 2, \ldots, 8$. Clearly, there is a natural grouping of obstacles where obstacles 3 and 4 are similar in the sense that they act practically as a single obstacle, since every trace passes either to the right or left of both. The same holds for pairs $(5, 6)$ and $(7, 8)$. Obstacles $1, 2$ are also similar in the sense that most traces behave similarly with respect to both, with only a few passing between them.

These intuitive results can be obtained from standard analytic and visualization methods. Figure 5(b) shows the correlation matrix of θ, where darker shades indicate higher correlation. The correlation lets us have a more abstract view of the domain, where related nearby holes can be viewed as one.

Techniques like Principal Component Analysis can be applied to the Euclidean data to determine which dimensions record larger variance – implying larger variability in how traces traverse the obstacles. We apply this idea to get the intuitive result in Figure 5(c) that obstacles 1 and 2 are clearly more significant than others as they split a large body of motions.

Greedy filtration of obstacles. A different strategy which is found effective in experiments, is to greedily select obstacles (dual sources) that maximize the accuracy for the task at hand.

For example, for nearest neighbor search, this accuracy can be defined as the fraction of times that the true Fréchet nearest neighbor is contained among the m nearest neighbors. The greedy strategy will iteratively select the obstacle that maximizes the total accuracy over all pairs, until it has selected some k obstacles. For scenarios with large number of obstacle, similar strategies can be implemented for distributed cluster computation [26]. The benefit of this heavy computation is that the signatures become more compact and assuming the dataset is representative of typical motion, future computations of signatures, nearest neighbors, predictions etc will be more efficient.

5.4 Adaptive resolution signatures

It is natural to ask for representations that give greater weight to recent information and less weight to history, for example, for short term prediction. The signatures can be seamlessly adapted to achieve this using weighted averaging. Where for each edge traversed by the trajectory, we modify the update rule to be $\theta_i(T) = \beta.\theta_i(T) + (1 - \beta)\xi_i(e)$ for a constant $\beta : 0 < \beta < 1$ that determines the weight of history in the signature.

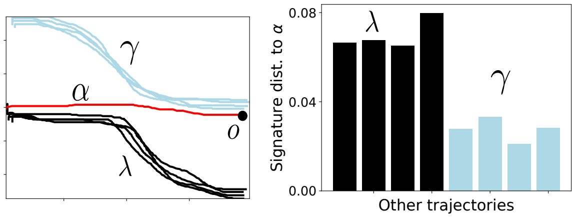

(a) (b)

Figure 6: (a) Trajectories flow left to right. (b) Distance of α's signature from others shows that in near future the set γ is more relevant than the set λ that have clearly diverged.

In the example in Figure 6(a) at point o, the adaptively weighted signature finds the set γ to be currently more relevant to the query α.

5.5 Composing signatures

The composability of differential forms means that a set of traces can be represented in the signature space as a linear combination of the constituent traces – such as the mean of all the signatures. This simplifies center computation by creating an abstract 'center' that is not a trajectory itself, but can be used to compare other trajectories to the given cluster or set.

5.6 Implementation in distributed and mobile setups

Mobile computers are a natural platform for application of trajectory signatures, with applications in social mobile networks, autonomous driving, etc. For large computers in automobiles, the differential forms can be pre-loaded into the memory, downloaded incrementally as required. In sensor or other dense network scenarios, the mobile device can obtain local values of ξ from nearby sensors and devices. The signature is computed and stored incrementally.

The knowledge of signatures allows mobile entities to exchange data with other nearby ones and predict which ones are likely to have similar behavior. This is useful, for example, in autonomous vehicles and delay tolerant networks.

The above constructions of differential forms are all naturally implementable in distributed scenarios like sensor networks. For example, consider a Voronoi diagram of sensors where they can detect the direction and identity of the objects crossing the edges of the voronoi graph, as used in [30]. The sensors maintain the weights on the edges giving the differential forms and as an object moves between cells, its signature is handed off (similar to hand-off in cellular network) to the successive sensor. An alternative approach could be for the sensors to record and store the edge crossings of mobile objects, and compute the signature on demand by summing along the handoff path.

6 EXPERIMENTS

In this section, we show experimental evidences that the topological signatures simplify the representation of trajectories and also perform well in clustering, prediction, and other tasks. The main observations are:

- Nearest neighbor of a query trajectory according to Fréchet distance can be found efficiently using fast Locality Sensitive Hashing and pruning on topological signatures.
- Motion prediction of trajectories is accurate and efficient. It achieves similar accuracy as Long Short Term Memory neural networks (henceforth LSTM), but provides much faster training and query time. Prediction results are verified using two real mobility datasets.
- Greedy source selection reduces dimension to get compact signatures, with minimal loss in quality of analytic results.
- Popular paths or paths with the most number of trajectories in a given region can be estimated by kernel density estimation on signatures.
- Topological signature based method is robust to sparse, noisy trajectories; it can predict future direction of mobile objects accurately in trajectories with many missing data points.

6.1 Experimental setup

Dataset. We use two publicly available datasets: Rome Taxi dataset [6] and Porto Dataset[1]. While the former has trajectories of 320 taxis for a month in Rome, Italy; the latter has trip partitioned trajectories of 442 taxis for one and half years in Porto, Portugal.

Constructing planar graph. The Delaunay triangulation [15] of 20000 random points in the plane make the planar graph G. Each gps point of a trajectory is mapped to its nearest node in G and connecting them by the shortest path in the graph produces its representation in G.

Identifying obstacles. All faces in G where less than a predefined threshold number of trajectories pass a boundary edge are considered as obstacles. E.g, the portion of Rome dataset in Figure 7(a) have 67 such obstacles with threshold 2. In Porto dataset (Figure 10(a)), we choose 30 largest regions of low trajectory density as obstacles.

Constructing differential forms. Dual paths along linear rays with random slopes from each obstacle yields the differential forms (Section 4.2). E.g, in both Figure 7(a) and Figure 10(a) 20 dual paths each with weight 0.05 are constructed from each obstacle.

6.2 Nearest neighbor search

Fréchet nearest neighbor of a query trajectory is approximated by the pruning based on LSH with trajectory signatures using independently chosen 3 sets of 5 linear projection hash functions. This experiment uses each trajectory in Figure 7(a) as a query trajectory in turn.

Figure 7(b) confirms that with high probability, Fréchet nearest neighbor is included in the approximate k nearest neighbors found by LSH. Larger bucket size naturally yields better accuracy and offers standard accuracy and efficiency trade-off of LSH.

In efficiency, even including preprocessing time to construct planar graph (15.9 sec), differential forms (20.5 sec), and computing signatures (varies with dataset size), this method greatly outperforms basic Fréchet based method of computing distance to all trajectories (Figure 7(c)). The Euclidean distance measure is faster than Fréchet and LSH based pruning makes a query even faster. Fréchet distance is computed using [1]. The experiments are run on a typical desktop machine with 8 GB primary memory and Intel $i5$ processor.

6.3 Clustering and estimating density

The signatures are useful to cluster trajectories. Figure 8 shows a small example with 66 trajectories. The varied types of trajectories are well separated even if they have large portion of overlapping pattern.

High density regions in the signature space correspond to popular topological types of trajectories. The popular bidirectional traffic flow in Figure 9(a) is neatly identifiable in the estimated density using Gaussian Kernel in Figure 9(b). Clustering can also be applied to anonymize personal data [37].

6.4 Motion prediction

Figure 7(a) and Figure 10(a) show the datasets from Rome and Porto respectively used in prediction experiments. With randomly chosen 90% trajectories as training, we predict direction ϕ for different scales r on each test trajectory where current location o is randomly chosen from middle 1/3rd of its length. The prediction error is measured as described in Section 5.2.

Using topological signatures, next direction is predicted as the mean direction ϕ of k nearest training trajectories that pass within 20 meters of o. The nearest neighbors are computed using kd-tree on the space of signatures with the training trajectory segments ending near o. In both Porto and Rome dataset, our method attains high accuracy even with small number of nearest neighbors (Figure 10(b)) and large prediction radius (Figure 11).

As a benchmark we use neural networks with LSTM as regressors [17] to predict ϕ, given equi-spaced 20 locations on the trajectory between o and start of the trajectory. Each model has two

[1] https://www.kaggle.com/c/pkdd-15-predict-taxi-service-trajectory-i

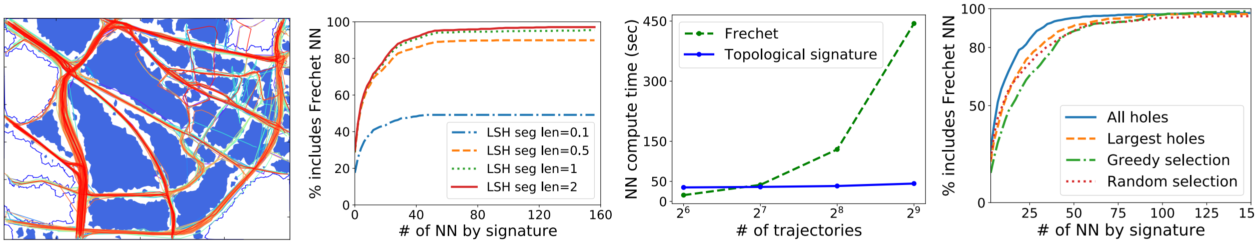

(a) (b) (c) (d)

Figure 7: (a) A region (latitude–$[41.8708°N, 41.8826°N]$ and longitude–$[12.4919°E, 12.5089°E]$) of size roughly $1km \times 1km$ from Rome taxi dataset with 1189 sub-trajectories. We detect 67 internal holes (shaded) using trajectory density threshold as 2.(b) CDF of percentage of times the nearest neighbor is included in the approximate k nearest neighbors (x-axis) found using Locality Sensitive Hashing based on topological signatures. With suitable segment length, Locality Sensitive Hashing can reliably approximate k nearest neighbors to find Fréchet based nearest neighbor. (c) Time to run naive Fréchet increases super linearly when increasing the size of the dataset whereas topological signature method consumes very little time in comparison. (d) k nearest neighbor query accuracy with 5 obstacles selected using different source selection strategies.

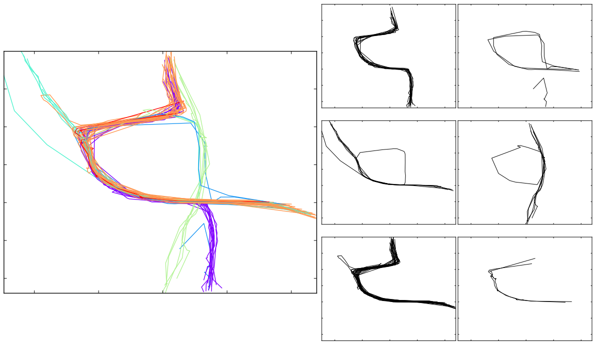

Figure 8: Clustering 66 trajectories from Rome taxi dataset using DBSCAN clustering algorithm with neighborhood distance parameter set as 0.25 and minimum samples to form a cluster is set as 2. To construct the triangulation, 20000 random points are used, Sources are placed based on the trajectory density threshold as 2.

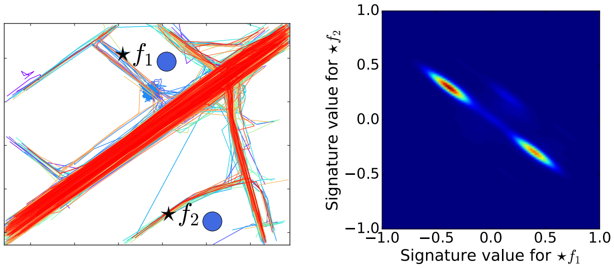

(a) (b)

Figure 9: Detecting popular topological types using kernel density estimate of the trajectory signatures. (a) Portion of trajectories from [6] with 1809 trajectories (area $1km \times 1km$). The busiest road in this map is easily visible. Two signature sources are manually placed in the map. (b) Two hotspots in the kernel density estimate denotes the two way traffic on the busy road.

layers of 20 LSTM cells followed by a fully connected layer with 100 rectified linear units. With a squared error loss function we train these models with a variant of stochastic gradient descent for 50 epochs using a batch size of 32 with the standard optimizer settings [13]. Figure 12(a) shows that simple k-NN on topological signatures achieve similar accuracy as LSTM, implying that the topological signatures in fact encode the critical intrinsic features that determine motion.

Figure 13 shows that topological signature based prediction is more efficient than LSTM in terms of both preprocessing and query time. Before answering queries, whereas our method requires to setup planar graph, identify obstacles, and create differential forms; LSTM requires data preprocessing and training. Although our method needs to find k nearest neighbors at query time, it offers faster query than LSTM. We use TensorFlow for implementing the LSTM [2]. All experiments are run on a typical desktop machine with 8 GB primary memory and Intel $i5$ processor.

Popular regression techniques, Random Forest, Gradient Boosting Trees, and Linear Regression also predict ϕ well given the current location o and topological signature of trajectory segments ending at o. High prediction accuracy of these methods in Figure 12(b) suggests that using topological signatures, the plethora of knowledge about these well studied methods can now be leveraged for trajectories and mobility analysis.

6.5 Signature source selection

In domains with large number of obstacles, the signatures will have correspondingly large size, losing the benefits of compact representation. We found that in practice, differential forms with respect to a small number of sources suffice to accurately capture the motion.

Figure 7(d) compares different signature source selection strategies in Rome dataset from Figure 7(a); different strategies can select small number of signature sources to attain high nearest neighbor query accuracy. Specifically, this experiment compares the following strategies: i) all faces in G with low trajectory density (holes) are signature sources, ii) k largest holes, iii) greedy selection as described in Section 5, and iv) randomly choose k sources from all

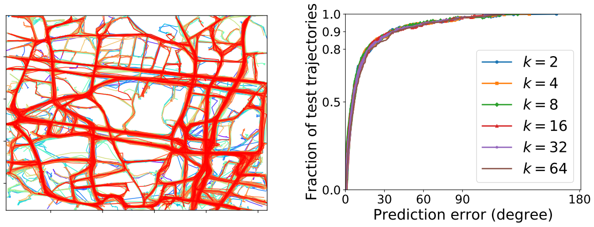

(a) (b)

Figure 10: (a) A region latitude–[$41.1468°N, 41.1699°N$] and longitude–[$8.62931°W, 8.60411°W$] of size $2.5Km \times 2.1Km$ from Porto dataset with 3952 trajectories. Among 101 regions with low trajectory density (threshold 2), we consider largest 30 to be obstacles. (b) In Porto dataset, topological signature based method accurately predicts next direction even with small number of nearest neighbors. Here, $r = 100$ meters.

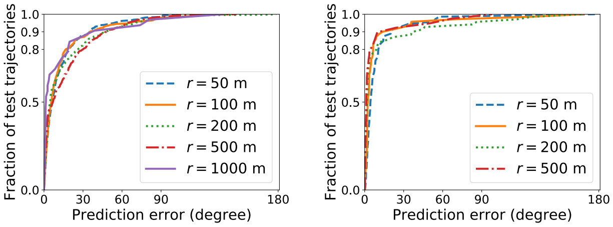

(a) (b)

Figure 11: Topological signature based method can accurately predict next direction even for large r in (a) Porto dataset and in (b) Rome dataset. Here, $k = 4$ neighbors.

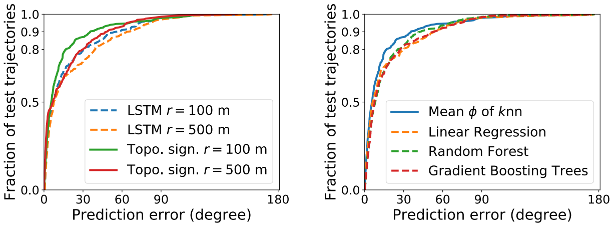

(a) (b)

Figure 12: (a) Topological signature based method attains similar accuracy as LSTM. (b) Popular regression methods using topological signatures achieve similar high accuracy.

faces in G. This result demonstrates that trajectories in a complex domain can be represented by simple low dimensional topological signatures.

6.6 Robustness to sparsity

Mobility traces differ in sparsity of constituent entities due to varied location sampling frequency. In this experiment, the dense GPS traces are made sparse by randomly retaining location points at fixed rates. The Figure 14 shows that our method can accurately predict motion in trajectories with missing locations.

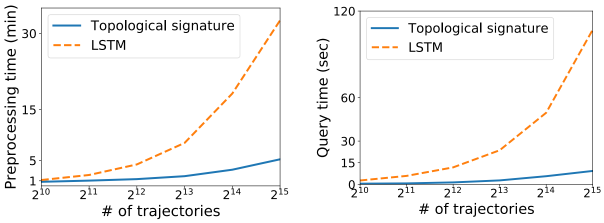

(a) (b)

Figure 13: (a) Preprocessing and (b) query time. Both increase slowly for topological signature based method compared to LSTM, with dataset size.

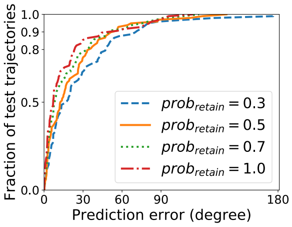

Figure 14: Predicting locations with sparse trajectories: Each location point is retained with certain probability in each trajectory. Our method achieves high prediction accuracy even with sparse trajectory.

7 RELATED WORK

Hodge decomposition of a randomly generated vector field has been used in [36] to classify paths into homotopy types. This approach relies on a numerical process, and only applies to trajectories with same start and end points. This problem is avoided to an extent in [28], which uses relative homology, and marks certain regions of the space where start and end points lie, but other trajectories do not pass. Thus these approaches do not apply to general trajectory datasets of the type we have considered here. Both these methods are also computationally expensive.

In other works, topological characterization has been used to measure distances between curves [10] but restricted to curves with same start and end points, since homotopy cannot be defined between open curves. A seminal work [5] Baryshnikov and Ghrist used integrals of Euler characteristics to compute number of mobile targets. Topological persistence can be used to simplify trajectories [22]. Discrete exterior calculus has been a subject of study in graphics, modeling and discrete geometry and developed in several different flavors [12, 19]. In sensor network, it has been used for performing range queries of mobile objects [30].

Mobility modeling using (hidden) Markov models have been developed in [24, 35, 38] and other works, usually with the objective to predict the agent's next road segment. As mentioned earlier, the Markov assumption can be shown to be unrepresentative of typical trajectory datasets [32]. In line with recent developments in machine learning, Neural networks have been designed for the prediction task. Recurrent Neural Networks using Long Short Term Memory are considered useful in sequential data, and has been used in [34]; we used a similar approach in our experiments, modified suitably for geometric trajectories in the datasets.

In contrast to these methods, our approach is computationally much more efficient in preprocessing, training as well as prediction query. It can be applied to road networks and geometric data alike. Unlike Markov and neural models that simply provide a prediction mechanism, the topological signatures reveal similarity between trajectories and reveal insights about how they traverse the domain. As a result, they can form the basis of search, clustering, prediction and other analytic tasks.

8 CONCLUSION

We presented a topological framework to represent a trajectory as a point in a Euclidean space, enabling natural applications of well established machine learning and mining techniques. The topological construct preserves relevant qualitative features in trajectories while ignoring the extraneous details and noise. The framework can be set up using fast distributed algorithms and used in an online manner by mobile entities. The framework is quite general and flexible, and it allows application specific choice of obstacles and domains. Dynamic obstacles, temporal characteristics of trajectories are interesting future directions to consider.

REFERENCES

[1] 2017. MDAnalysis 0.16.2. (2017). http://www.mdanalysis.org/.

[2] Martín Abadi, Paul Barham, Jianmin Chen, Zhifeng Chen, Andy Davis, Jeffrey Dean, Matthieu Devin, Sanjay Ghemawat, Geoffrey Irving, Michael Isard, and others. 2016. TensorFlow: A System for Large-Scale Machine Learning.. In *OSDI*, Vol. 16. 265–283.

[3] Helmut Alt and Michael Godau. 1995. Computing the Fréchet distance between two polygonal curves. *International Journal of Computational Geometry & Applications* 5, 01n02 (1995), 75–91.

[4] Maria Astefanoaei, Paul Cesaretti, Panagiota Katsikouli, Mayank Goswami, and Rik Sarkar. 2018. Multi-resolution sketches and locality sensitive hashing for fast trajectory processing. In *26th ACM SIGSPATIAL International Conference on Advances in Geographic Information Systems (ACM SIGSPATIAL)*.

[5] Yuliy Baryshnikov and Robert Ghrist. 2009. Target enumeration via Euler characteristic integrals. *SIAM J. Appl. Math.* 70, 3 (2009), 825–844.

[6] Lorenzo Bracciale, Marco Bonola, Pierpaolo Loreti, Giuseppe Bianchi, Raul Amici, and Antonello Rabuffi. 2014. CRAWDAD data set roma/taxi (v. 2014-07-17). *July* (2014).

[7] Kevin Buchin, Maike Buchin, Marc Van Kreveld, Maarten Löffler, Rodrigo I Silveira, Carola Wenk, and Lionov Wiratma. 2013. Median trajectories. *Algorithmica* 66, 3 (2013), 595–614.

[8] Lili Cao and John Krumm. 2009. From GPS traces to a routable road map. In *Proceedings of the 17th ACM SIGSPATIAL international conference on advances in geographic information systems*. ACM, 3–12.

[9] Erin Wolf Chambers, Eric Colin De Verdiere, Jeff Erickson, Sylvain Lazard, Francis Lazarus, and Shripad Thite. 2010. Homotopic Fréchet distance between curves or, walking your dog in the woods in polynomial time. *Computational Geometry* 43, 3 (2010), 295–311.

[10] Erin Wolf Chambers and Yusu Wang. 2013. Measuring similarity between curves on 2-manifolds via homotopy area. In *Proceedings of the twenty-ninth annual symposium on Computational geometry*. ACM, 425–434.

[11] Mayur Datar, Nicole Immorlica, Piotr Indyk, and Vahab S Mirrokni. 2004. Locality-sensitive hashing scheme based on p-stable distributions. In *Proceedings of the twentieth annual symposium on Computational geometry*. ACM, 253–262.

[12] Mathieu Desbrun, Eva Kanso, and Yiying Tong. 2008. Discrete differential forms for computational modeling. In *Discrete differential geometry*. Springer, 287–324.

[13] Jimmy Ba Diederik P. Kingma. 2015. Adam: A Method for Stochastic Optimization. In *Proceedings of the 3rd International Conference on Learning Representations (ICLR) (ICLR '15)*.

[14] Anne Driemel and Francesco Silvestri. 2017. Locality-Sensitive Hashing of Curves. In *33rd International Symposium on Computational Geometry (SoCG 2017)*, Vol. 77. 37:1–37:16.

[15] Herbert Edelsbrunner and John Harer. 2010. *Computational topology: an introduction.* American Mathematical Soc.

[16] Stefan Funke and Nikola Milosavljevic. 2007. Network sketching or: How Much Geometry Hides in Connectivity?–Part II. In *Proceedings of the eighteenth annual ACM-SIAM symposium on Discrete algorithms*. Society for Industrial and Applied Mathematics, 958–967.

[17] Felix A Gers, Jürgen Schmidhuber, and Fred Cummins. 1999. Learning to forget: Continual prediction with LSTM. (1999).

[18] John Hershberger and Jack Snoeyink. 1994. Computing minimum length paths of a given homotopy class. *Computational geometry* 4, 2 (1994), 63–97.

[19] Anil Nirmal Hirani. 2003. *Discrete exterior calculus.* Ph.D. Dissertation. California Institute of Technology.

[20] Piotr Indyk. 2002. Approximate nearest neighbor algorithms for Fréchet distance via product metrics. In *Proceedings of the eighteenth annual symposium on Computational geometry*. ACM, 102–106.

[21] Panagiota Katsikouli, Maria Astefanoaei, and Rik Sarkar. 2018. Distributed Mining of Popular Paths in Road Networks. In *DCOSS 2018-International Conference on Distributed Computing in Sensor Systems*. IEEE, 1–8.

[22] Panagiota Katsikouli, Rik Sarkar, and Jie Gao. 2014. Persistence based online signal and trajectory simplification for mobile devices. In *Proceedings of the 22nd ACM SIGSPATIAL International Conference on Advances in Geographic Information Systems*. ACM, 371–380.

[23] L Christine Kinsey. 2012. *Topology of surfaces.* Springer Science & Business Media.

[24] Tong Liu, Paramvir Bahl, and Imrich Chlamtac. 1998. Mobility modeling, location tracking, and trajectory prediction in wireless ATM networks. *IEEE Journal on selected areas in communications* 16, 6 (1998), 922–936.

[25] Jianming Lv, Qing Li, Qinghui Sun, and Xintong Wang. 2018. T-CONV: A Convolutional Neural Network For Multi-scale Taxi Trajectory Prediction. In *Big Data and Smart Computing (BigComp), 2018 IEEE International Conference on*. IEEE, 82–89.

[26] Baharan Mirzasoleiman, Amin Karbasi, Rik Sarkar, and Andreas Krause. 2016. Distributed submodular maximization. *The Journal of Machine Learning Research* 17, 1 (2016), 8330–8373.

[27] Badri Nath and Dragoş Niculescu. 2003. Routing on a curve. *ACM SIGCOMM Computer Communication Review* 33, 1 (2003), 155–160.

[28] Florian T Pokorny, Ken Goldberg, and Danica Kragic. 2016. Topological trajectory clustering with relative persistent homology. In *Robotics and Automation (ICRA), 2016 IEEE International Conference on*. IEEE, 16–23.

[29] Hiroaki Sakoe and Seibi Chiba. 1978. Dynamic programming algorithm optimization for spoken word recognition. *Acoustics, Speech and Signal Processing, IEEE Transactions on* 26, 1 (1978), 43–49.

[30] Rik Sarkar and Jie Gao. 2013. Differential forms for target tracking and aggregate queries in distributed networks. *IEEE/ACM Transactions on Networking (TON)* 21, 4 (2013), 1159–1172.

[31] Rik Sarkar, Xiaotian Yin, Jie Gao, Feng Luo, and Xianfeng David Gu. 2009. Greedy routing with guaranteed delivery using ricci flows. In *Information Processing in Sensor Networks, 2009. IPSN 2009. International Conference on*. IEEE, 121–132.

[32] Mudhakar Srivatsa, Raghu Ganti, Jingjing Wang, and Vinay Kolar. 2013. Map matching: Facts and myths. In *Proceedings of the 21st ACM SIGSPATIAL International Conference on Advances in Geographic Information Systems*. ACM, 484–487.

[33] Yue Wang, Jie Gao, and Joseph SB Mitchell. 2006. Boundary recognition in sensor networks by topological methods. In *Proceedings of the 12th annual international conference on Mobile computing and networking*. ACm, 122–133.

[34] Hao Wu, Ziyang Chen, Weiwei Sun, Baihua Zheng, and Wei Wang. 2017. Modeling trajectories with recurrent neural networks. IJCAI.

[35] Andy Yuan Xue, Rui Zhang, Yu Zheng, Xing Xie, Jin Huang, and Zhenghua Xu. 2013. Destination prediction by sub-trajectory synthesis and privacy protection against such prediction. In *Data Engineering (ICDE), 2013 IEEE 29th International Conference on*. IEEE, 254–265.

[36] Xiaotian Yin, Chien-Chun Ni, Jiaxin Ding, Wei Han, Dengpan Zhou, Jie Gao, and Xianfeng David Gu. 2015. Decentralized human trajectories tracking using hodge decomposition in sensor networks. In *Proceedings of the 23rd SIGSPATIAL International Conference on Advances in Geographic Information Systems*. ACM, 54.

[37] Jiemin Zeng, Gaurish Telang, Matthew P Johnson, Rik Sarkar, Jie Gao, Esther M Arkin, and Joseph SB Mitchell. 2017. Mobile r-gather: Distributed and geographic clustering for location anonymity. In *Proceedings of the 18th ACM International Symposium on Mobile Ad Hoc Networking and Computing*. ACM.

[38] Brian D Ziebart, Andrew L Maas, J Andrew Bagnell, and Anind K Dey. 2008. Maximum Entropy Inverse Reinforcement Learning.. In *AAAI*, Vol. 8. Chicago, IL, USA, 1433–1438.